Structural, Electronic, and Mechanical Properties of Anatase and Rutile Titanium Dioxide Phases using the Density Functional Theory

Asma A. Al-Enzi
Department of Physics, College of Science, Northern Border University, Arar, Saudi Arabia
st202003731@stu.nbu.edu.sa

Omer I. Eid
Department of Physics, College of Science, Northern Border University, Arar, Saudi Arabia | Department of Physics, Faculty of Science, University of Khartoum, Sudan
omer.hassin@nbu.edu.sa, omereid@gmail.com (corresponding author)

M. E. M. Eisa
Department of Physics, College of Science, Northern Border University, Arar, Saudi Arabia | Department of Physics, College of Science, Sudan University of Science and Technology, Sudan
memeisa@gmail.com

Received: 14 July 2024 | Revised: 30 July 2024 and 4 August 2024 | Accepted: 11 August 2024

 DOI: https://doi.org/10.48084/etasr.8393

ABSTRACT

This study investigates the structural and electronic properties of the anatase and rutile TiO_2 systems by employing the Quantum Espresso (QE) software using first-principles calculations based on Density Functional Theory (DFT). Optimized lattice constants (a = 3.788, 4.627 a.u. and c = 9.491, 2.979 a.u.) and the internal parameter u (0.209, 0.305), were obtained for anatase and rutile TiO_2 phases, respectively. Unit cell volumes were also calculated. Furthermore, the Birch-Murnaghan equation of state was used to obtain the equilibrium volume (937.5, 428.3 a.u.^{3}), the bulk modulus (198.5, 222.5 GPa), and the pressure derivative of the bulk modulus (4.18, 4.37) for both phases. The results are in good agreement with the experimental data and the theoretical results published in other studies. Finally, the energy band gap of both samples was calculated (1.8 and 1.6 eV, respectively) and compared with published results obtained from the Density Of Electron States (DOS).

Keywords-titanium dioxide; anatase; rutile; DFT; electronic structure; energy band gap; bulk modulus

I. INTRODUCTION

Titanium dioxide has been extensively studied for its interesting electrical [1-2], electronic, and structural properties, both experimentally [3-6] and theoretically [7-9]. In addition to its usage as alloy sheets [10-12] and the experimental investigation of the dielectric properties of PVC films doped with TiO_2 [13]. In [14], the photocatalytic and magnetic properties of TiO_2 were studied. Its applications extend to solar cell structures, where it is used as an excellent transport layer [15]. In an ab initio study in [16], various properties of anatase titanium dioxide nanoparticles were investigated. This study provided some empirical insight into how the mechanical properties of anatase improved by implementing the Linear Combinations of Atomic Orbitals (LCAO) method. In [17], a pressure-induced study of the structural and electronic bandgap properties of anatase and rutile was conducted using the ultrasoft pseudopotential plane-wave method. Both anatase and rutile TiO_2 have a tetragonal crystal structure, I41/amd and P42/mnm space groups, respectively. The Density-Functional Theory (DFT) is used in simulation programs. In [18], an X-Ray Diffraction (XRD) study was performed, and the lattice parameters of anatase were experimentally determined as a=3.7842 Å, c=9.4938 Å. For rutile, the parameters were given in [19] as a=4.5938 Å and c=2.9586 Å.

II. COMPUTATIONAL METHOD AND SIMULATIONS

This study was performed using Plane-Wave self-consistent field (PWscf), an essential component of QE within the DFT

framework [20-21]. In addition to scf calculations, non-self-consistent field (nscf) calculations were performed. Furthermore, the dos card, available within the QE code, was used to calculate the Density Of Electron States (DOS). The energy-volume (ev) tool was also used to calculate the bulk modulus from the total energy and unit cell volume values. The pseudopotentials employed in this study were the ultrasoft pseudopotentials (PP) "Ti.pw91-sp-van_ak.UPF" for titanium and "O.pw91-van_ak.UPF" for oxygen, with the Perdew-Wang 91 gradient-corrected function type following the Vanderbilt ultrasoft method [22]. DFT is commonly employed in the investigation of the structural properties of alkali metal hydrides [23].

A. K-Points Mesh Test

To choose the correct set of k-points for accurate calculations, convergence tests concerning the total energy were performed for different k-point grids. For Monkhorst-Pack [24] grid parameters (nk_1 + nk_2 +nk_3), the k's were kept equal to one and varied n from 2 to 10. This was done at first to have a general idea about the total number of points needed. The second step was to test the z-direction separately since the anatase unit cell is longer along the z-direction compared to x- and y-directions, therefore, fewer k-points are needed in the z-direction. This is because the dimension in the reciprocal lattice is inversely proportional to the dimension in the real space. Hence, to attain matching density in the x- and y-axis, fewer k-points are needed in the z-direction. The rutile unit cell is shorter along the z-axis, so more k-points are needed in this direction. The last step in the k-points test was to test the x- and y- directions keeping the selected number of points in the z-direction unaltered. According to the tests, a grid of 8×8×4 k-points was chosen for the anatase and 5×5×9 k-points for the rutile, as shown in Figures 1 and 2, respectively.

As can be inferred from Figures 1 and 2, the total energy decreases as n increases. The convergence threshold on the total energy was set to 10^{-4} Ry as a stop condition for the iteration. However, the difference in the energy is not significant after the k-points mesh (8×8×4) for anatase and (5×5×9) for rutile. This encouraged us to choose these sets as the finest k-points grids in the scf calculations.

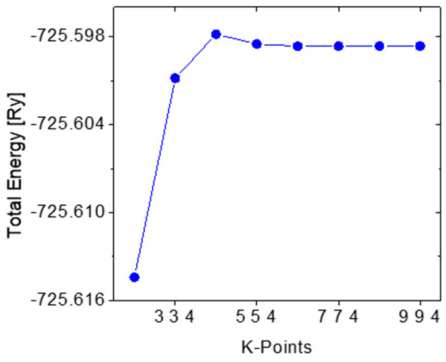

Fig. 1. The total energy (Ry) of the anatase phase versus the n×n×4 k-points grid.

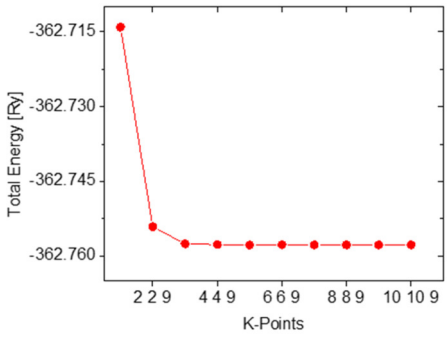

Fig. 2. The total energy (Ry) of the rutile phase versus the n×n×9 k-points grid.

B. Plane Wave Cutoff Test

Optimization of kinetic energy cutoff was performed to limit the number of plane waves whose energy is less than or equal to the kinetic energy shift. This is necessary to achieve accurate computational results. To ensure convergence of the total energy with the kinetic energy cutoff for wavefunctions (ecutwfc), a series of calculations of the total energy of unrelaxed anatase and rutile unit cells were performed via a range of cutoff energies starting from 20 to 120 Ry in steps of 20 Ry. The results are shown in Figures 3 and 4 for anatase and rutile, respectively. As a condition for the iteration to stop, the convergence threshold on total energy was set to 10^{-4} Ry. Note that the energy difference between ecutwfc 80 Ry and 90 Ry is significantly very small. This is why the value of 80 Ry was accepted as an optimum value for ecutwfc in simulations.

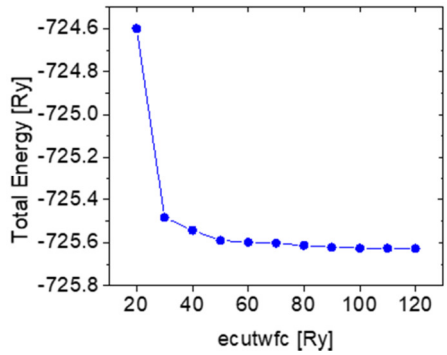

Fig. 3. The total energy convergence versus the kinetic energy cut-off for the wavefunctions of anatase.

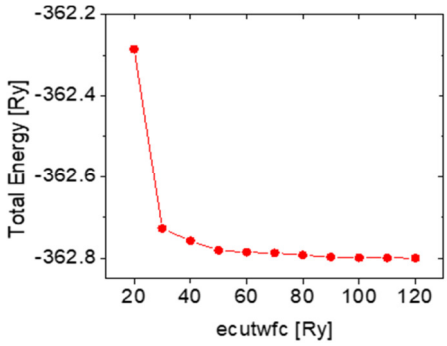

Fig. 4. The total energy convergence versus the kinetic energy cut-off for the wavefunctions of rutile.

III. RESULTS AND DISCUSSION

A. Structural Optimization

Keeping the optimal values of ecutwfc (80 Ry) and the k-points sets for anatase (8×8×4) and rutile (5×5×9), simulations were carried out for different values of the cell lattice constant while keeping the lattice ratio (i.e., the c-axis length to the a-axis length in the tetragonal lattice) unaltered. The scf code was executed for different values of the cell lattice constant, 7.1507 ± 01 a.u. and 8.6814 ± 0.1 a.u. for anatase and rutile, respectively. The resulting total energies versus the cell lattice values were then graphed and fitted using a standard cubic equation. The fitting parameters showed that the minimum total energy was achieved when the lattice constant value was 7.1732 a.u. and 8.7384, i.e., with only a 0.3% and 0.6% error of the experimental values for anatase and rutile, respectively.

B. Relaxed State

QE was used for variable cell calculations to optimize the atomic coordinates, atomic positions, and volume of the unit cell by minimizing the total energy and atomic forces to obtain accurate results. Figure 5 presents the relaxed lattice cells of anatase and rutile with the help of the xcrysden software [25]. Table I shows the optimized structural parameters a, b, c, and u (the internal parameter) calculated for both anatase and rutile. As can be observed, the calculated structural parameters for both anatase and rutile agree very well with the experimental values. The optimized parameters for anatase agree well with the experimental values and are better than some previous theoretical results, for instance, the results obtained in [26] by employing the Full-Potential Linearized Augmented Plane-Wave (FLAPW) method. However, in [17], the pressure-induced structural and electronic bandgap properties of anatase and rutile TiO_2 were studied using the GGA proposed by Perdew-Burke-Ernzerhof (PBE) for the exchange-correlation potential, obtaining an overestimated value for the lattice constant c=9.852 Å (0.181 Å difference). However, the other parameters agreed well with those of this study for anatase.

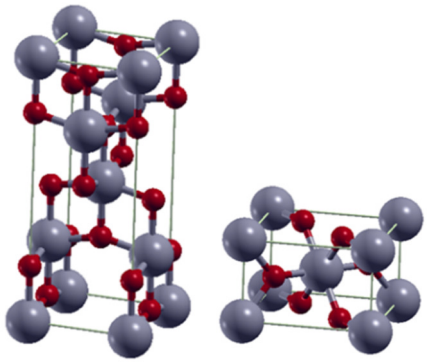

(a) (b)

Fig. 5. Anatase (a) and rutile (b) relaxed structures. Red represents an oxygen atom.

Furthermore, as shown in Table I, the structural parameter values for rutile TiO_2 follow the experimental data better than the theoretical studies mentioned.

C. Bulk Modulus and Equation of State

To obtain the bulk modulus value, the ev.x (energy versus volume) package of QE was used, which allows to calculate the bulk modulus for the relaxed system using the Birch-Murnaghan equation of state [28]. Several scf input files were compiled with different values of lattice parameters. Then from the output files, the total energy values at different volumes of the unit cell were collected in a new input file and executed using ev.x. Table II shows the output values of the bulk modulus, the pressure derivative of the bulk modulus, and the equilibrium volume of the unit cell for both anatase and rutile.

TABLE I. OPTIMIZED LATTICE PARAMETERS FOR ANATASE AND RUTILE OF TIO_2 PHASES: EXPERIMENTAL AND THEORETICAL VALUES

Sample	Parameter	Experimental Data	This study	Other works	
				FLAPW [26]	GGA-PBE [11]
Anatase	a (Å)	3.784 [18, 19]	3.788	3.692	3.798
	c (Å)	9.494 [18, 19]	9.491	9.471	9.852
	u	0.208 [27]	0.209	0.206	0.206
Rutile	a (Å)	4.594 [18, 19]	4.627	4.656	4.705
	c (Å)	2.959 [18, 19]	2.979	2.967	2.966
	u	0.305 [27]	0.305	0.305	0.308

TABLE II. COMPUTED AND EXPERIMENTAL VALUES OF BULK MODULUS (B_0), BULK MODULUS DERIVATIVE (B_0'), AND UNIT CELL VOLUME (V_0) OF ANATASE AND RUTILE

Sample	Parameter	This study		Experimental data [29]	Other theoretical studies	
		Fitting	ev package		GGA-PBE [17]	GGA-PW91 [30]
Anatase	B_o (GPa)	205.9	198.5	179	188	146.0
	B_o'	4.24	4.18	4.5	3.7	4.0
	V_o (a.u.)^3	936.6	937.5	919.7	959.3	908.1
Rutile						GGA-PBE [31]
	B_o (GPa)	228.0	222.5	211	244	210
	B_o'	4.3	4.37	6.5	3.6	5.8
	V_o (a.u.)^3	428.4	428.3	421.4	443.2	413.6

Furthermore, another method was used to calculate the bulk modulus by running several scf files with the optimized values obtained from vc-relax calculations. Then the total energies and the unit cell volumes were collected for different input values

of the lattice parameters. Afterward, the Birch-Murnaghan equation of state [28] was used to fit the calculated total energies at various unit-cell volumes. The main difference between the two methods is that the first one (ev.x) did not require running the optimization process using vc-relax. This is shown in Figures 6 and 7 for anatase and rutile, respectively. The value of the pressure derivative (B_o') was assumed to be not less than 4 in this fitting. The results are shown in Table II along with the experimental data and other theoretical values obtained by employing different computational methods.

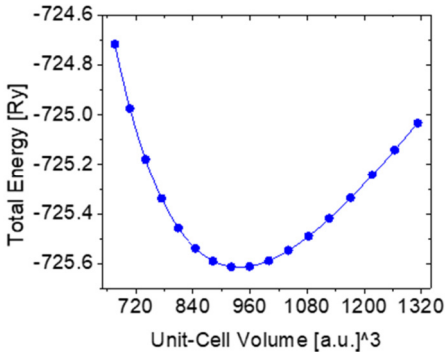

Fig. 6. The total energy versus the unit cell volume of the anatase phase. The line represents the fitted data using the equation of state.

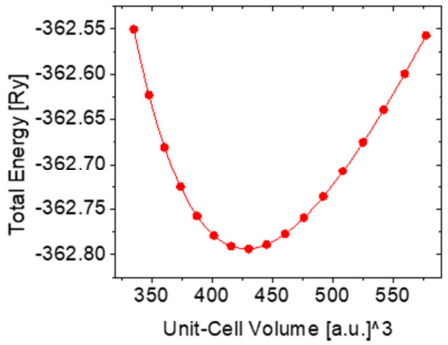

Fig. 7. The total energy versus the unit cell volume of the rutile phase. The line represents the fitted data using the equation of state.

From the data shown in Table II, it is clear that both methods, ev.x tool and the direct use of the equation of state, used to fit the total energy concerning the unit-cell volume yielded close values. For example, considering anatase, the difference in the bulk modulus values between the two methods is only 7.4 GPa. Although both values are slightly larger compared to the experimental data, the value obtained using the ev feature is better compared to the one revealed by the fitting. The study in [11], which used the GGA-PBE method, recorded better values for anatase but overestimated the unit cell volume value. The rutile data in this study are much closer to the experimental values. Compared to [30], which used the PW91-GGA method, the values calculated in this study are better. In [31], GGA parameterized by PBE was used, obtaining a better value for the bulk modulus of rutile, but it undervalued the unit cell volume.

D. Density of States

Figures 8 and 9 show the calculated density of electron states in anatase and rutile, respectively. The oxygen 2s-states are located in the band between -18 and -15 eV, while the 2p-states band, which covers the range -5 to 0 eV, represents the valence band. The conduction band, which consists mostly of the titanium 3d-states, spreads in the range of 2 to 5 eV, away from the valence band by about 1.8 eV for anatase and 1.6 eV for rutile. These values represent the energy band gaps calculated in this study. It can be noticed that the energy band gap values are underestimated compared to the experimental values reported in [32], which were 3.20 eV for anatase and 3.03 eV for rutile. This is a known disadvantage of DFT calculations, as, in general, DFT-calculated energy bandgaps are critically underestimated [33, 34]. The disagreement reported in the literature reaches 50%. However, in [35], a large-scale DFT study was conducted on the influence of the exchange-correlation function in the calculation of electronic band gaps of solids. This study identified optimal parameters that yield a family of functions adapted for the calculation of energy bandgaps.

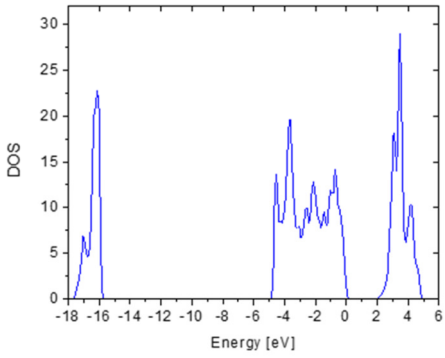

Fig. 8. Density of electron states in anatase optimized using QE.

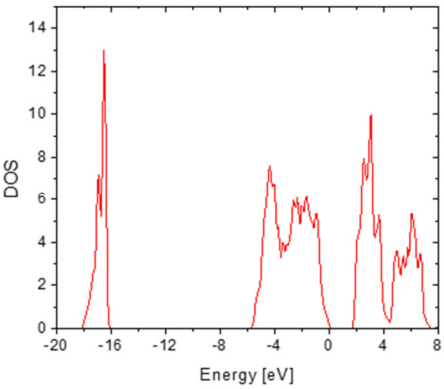

Fig. 9. Density of electron states of rutile optimized using QE.

In an ab initio study of excited electron dynamics in anatase and rutile [36], a value of 1.5 eV energy band gap was recorded for both titanium dioxide phases. In another computational study [37], 2.04 eV was achieved for anatase and 1.78 eV for rutile. The data in these studies were better than those in this study, but still very low compared to the experimental data.

IV. CONCLUSION

This study used the DFT method and Quantum ESPRESSO (QE) open-source software to investigate the structural and mechanical properties of the anatase and rutile titanium dioxide (TiO_2) phases. The results include optimized structures and lattice parameters (a = 3.788, 4.627 a.u. and c = 9.491, 2.979 a.u. and u = 0.209, 0.305), minimum unit cell volumes (937.5, 428.3 a.u.^{3}), bulk modulus and its derivative (198.5, 222.5 GPa and 4.18, 4.37), and energy band gaps (1.8, 1.6 eV), for anatase and rutile, respectively. The importance of this study is evident in the accurate measurements, which agree well with the published experimental and theoretical results, demonstrating the accuracy and reliability of the computational method. Furthermore, this study provides important information regarding the mechanical properties of anatase and rutile. This is significant for understanding how these materials can be used in structural and engineering applications. This study relates to previous ones, and therefore, its findings are comparable with the experimental data and show good agreement. This verification is an important step in computational materials science. This study contributes to the literature and provides detailed and consistent information on the mechanical properties of anatase and rutile TiO_2. However, it is recommended to consider the approach in [35] when investigating bandgaps, which used other functions specifically designed for this purpose. A proposed evaluation of this method to calculate the bandgaps opens the way for future research to polish the current findings.

ACKNOWLEDGEMENTS

The authors acknowledge the Deanship of Scientific Research at Northern Border University, Arar, KSA for funding this research work through project no. NBU-FFR-2024-1956-01. Asma Al-Enzi would like to express her sincere gratitude and appreciation for being granted the M.Sc. Scholarship from Northern Border University.

REFERENCES

[1] T. Ji *et al.*, "Effect of Grain Size on Electrical Properties of Anatase TiO_2 under High Pressure," *The Journal of Physical Chemistry C*, vol. 125, no. 6, pp. 3314–3319, Feb. 2021, https://doi.org/10.1021/acs.jpcc.0c10934.

[2] J. Reintjes and M. B. Schulz, "Photoelastic Constants of Selected Ultrasonic Delay-Line Crystals," *Journal of Applied Physics*, vol. 39, no. 11, pp. 5254–5258, Oct. 1968, https://doi.org/10.1063/1.1655948.

[3] W. Göpel *et al.*, "Surface defects of TiO2(110): A combined XPS, XAES AND ELS study," *Surface Science*, vol. 139, no. 2, pp. 333–346, Apr. 1984, https://doi.org/10.1016/0039-6028(84)90054-2.

[4] A. F. Carley, P. R. Chalker, J. C. Riviere, and M. W. Roberts, "The identification and characterisation of mixed oxidation states at oxidised titanium surfaces by analysis of X-ray photoelectron spectra," *Journal of the Chemical Society, Faraday Transactions 1: Physical Chemistry in Condensed Phases*, vol. 83, no. 2, pp. 351–370, Jan. 1987, https://doi.org/10.1039/F19878300351.

[5] B. W. Veal and A. P. Paulikas, "Final-state screening and chemical shifts in photoelectron spectroscopy," *Physical Review B*, vol. 31, no. 8, pp. 5399–5416, Apr. 1985, https://doi.org/10.1103/PhysRevB.31.5399.

[6] R. Brydson, H. Sauer, W. Engel, and F. Hofer, "Electron energy-loss near-edge structures at the oxygen K edges of titanium(IV) oxygen compounds," *Journal of Physics: Condensed Matter*, vol. 4, no. 13, Nov. 1992, Art. no. 3429, https://doi.org/10.1088/0953-8984/4/13/007.

[7] K. M. Glassford and J. R. Chelikowsky, "Electronic structure of TiO_2:Ru," *Physical Review B*, vol. 47, no. 19, pp. 12550–12553, May 1993, https://doi.org/10.1103/PhysRevB.47.12550.

[8] D. Vogtenhuber, R. Podloucky, A. Neckel, S. G. Steinemann, and A. J. Freeman, "Electronic structure and relaxed geometry of the TiO_2 rutile (110) surface," *Physical Review B*, vol. 49, no. 3, pp. 2099–2103, Jan. 1994, https://doi.org/10.1103/PhysRevB.49.2099.

[9] A. Fahmi, C. Minot, B. Silvi, and M. Causá, "Theoretical analysis of the structures of titanium dioxide crystals," *Physical Review B*, vol. 47, no. 18, pp. 11717–11724, May 1993, https://doi.org/10.1103/PhysRevB.47.11717.

[10] D. Aroussi, B. Aour, and A. S. Bouaziz, "A Comparative Study of 316L Stainless Steel and a Titanium Alloy in an Aggressive Biological Medium," *Engineering, Technology & Applied Science Research*, vol. 9, no. 6, pp. 5093–5098, Dec. 2019, https://doi.org/10.48084/etasr.3208.

[11] A. Boudjemline, M. Boujelbene, and E. Bayraktar, "Surface Quality of Ti-6Al-4V Titanium Alloy Parts Machined by Laser Cutting," *Engineering, Technology & Applied Science Research*, vol. 10, no. 4, pp. 6062–6067, Aug. 2020, https://doi.org/10.48084/etasr.3719.

[12] V. C. Nguyen, T. D. Nguyen, and D. H. Tien, "Cutting Parameter Optimization in Finishing Milling of Ti-6Al-4V Titanium Alloy under MQL Condition using TOPSIS and ANOVA Analysis," *Engineering, Technology & Applied Science Research*, vol. 11, no. 1, pp. 6775–6780, Feb. 2021, https://doi.org/10.48084/etasr.4015.

[13] L. Madani, K. S. Belkhir, and S. Belkhiat, "Experimental Study of Electric and Dielectric Behavior of PVC Composites," *Engineering, Technology & Applied Science Research*, vol. 10, no. 1, pp. 5233–5236, Feb. 2020, https://doi.org/10.48084/etasr.3246.

[14] T. Gegechkori, G. Mamniashvili, T. Gagnidze, M. Nadareishvili, and T. Zedginidze, "Photocatalytic and Magnetic Properties of TiO2 Micro- and Nano- Powders decorated by Magnetic Cocatalysts," *Engineering, Technology & Applied Science Research*, vol. 13, no. 5, pp. 11924–11931, Oct. 2023, https://doi.org/10.48084/etasr.6244.

[15] M. Oproescu, A. G. Schiopu, V. M. Calinescu, V. G. Iana, N. Bizon, and M. Sallah, "Influence of Supplementary Oxide Layer on Solar Cell Performance," *Engineering, Technology & Applied Science Research*, vol. 14, no. 2, pp. 13274–13282, Apr. 2024, https://doi.org/10.48084/etasr.6879.

[16] D. Dash, C. K. Pandey, S. Chaudhary, and S. K. Tripathy, "Structural, electronic, and mechanical properties of anatase titanium dioxide: An ab-initio approach," *Multidiscipline Modeling in Materials and Structures*, vol. 15, no. 2, pp. 306–316, Jan. 2018, https://doi.org/10.1108/MMMS-03-2018-0043.

[17] T. Mahmood *et al.*, "Pressure Induced Structural and Electronic Bandgap properties of Anatase and Rutile TiO_2," *Sains Malaysiana*, vol. 42, no. 2, pp. 231–237, 2013.

[18] W. Zhang, T. Hu, B. Yang, P. Sun, and H. He, "The Effect of Boron Content on Properties of B-TiO_2 Photocatalyst Prepared by Sol-gel Method," *Journal of Advanced Oxidation Technologies*, vol. 16, no. 2, pp. 261–267, Jul. 2013, https://doi.org/10.1515/jaots-2013-0206.

[19] D. G. Isaak, J. D. Carnes, O. L. Anderson, H. Cynn, and E. Hake, "Elasticity of TiO2 rutile to 1800 K," *Physics and Chemistry of Minerals*, vol. 26, no. 1, pp. 31–43, Nov. 1998, https://doi.org/10.1007/s002690050158.

[20] P. Giannozzi *et al.*, "QUANTUM ESPRESSO: a modular and open-source software project for quantum simulations of materials," *Journal of Physics: Condensed Matter*, vol. 21, no. 39, Jun. 2009, Art. no. 395502, https://doi.org/10.1088/0953-8984/21/39/395502.

[21] P. Giannozzi *et al.*, "Quantum ESPRESSO toward the exascale," *The Journal of Chemical Physics*, vol. 152, no. 15, Apr. 2020, Art. no. 154105, https://doi.org/10.1063/5.0005082.

[22] "Pseudopotentials," *Quantum Espresso*. https://www.quantum-espresso.org/pseudopotentials/.

[23] T. Iliass, H. Ziani, A. Gueddim, and A. D. Guibadj, "DFT Investigation of the Structual and Optoelectronic Properties of Alkali Metal Hydrides MH (M=Li, Na)," *Engineering, Technology & Applied Science Research*, vol. 12, no. 1, pp. 8151–8156, Feb. 2022, https://doi.org/10.48084/etasr.4645.

[24] H. J. Monkhorst and J. D. Pack, "Special points for Brillouin-zone integrations," *Physical Review B*, vol. 13, no. 12, pp. 5188–5192, Jun. 1976, https://doi.org/10.1103/PhysRevB.13.5188.

[25] A. Kokalj, "XCrySDen-a new program for displaying crystalline structures and electron densities," *Journal of Molecular Graphics and Modelling*, vol. 17, no. 3, pp. 176–179, Jun. 1999, https://doi.org/10.1016/S1093-3263(99)00028-5.

[26] R. Asahi, Y. Taga, W. Mannstadt, and A. J. Freeman, "Electronic and optical properties of anatase TiO_2," *Physical Review B*, vol. 61, no. 11, pp. 7459–7465, Mar. 2000, https://doi.org/10.1103/PhysRevB.61.7459.

[27] J. K. Burdett, T. Hughbanks, G. J. Miller, J. W. Jr. Richardson, and J. V. Smith, "Structural-electronic relationships in inorganic solids: powder neutron diffraction studies of the rutile and anatase polymorphs of titanium dioxide at 15 and 295 K," *Journal of the American Chemical Society*, vol. 109, no. 12, pp. 3639–3646, Jun. 1987, https://doi.org/10.1021/ja00246a021.

[28] F. D. Murnaghan, "The Compressibility of Media under Extreme Pressures," *Proceedings of the National Academy of Sciences*, vol. 30, no. 9, pp. 244–247, Sep. 1944, https://doi.org/10.1073/pnas.30.9.244.

[29] T. Arlt *et al.*, "High-pressure polymorphs of anatase TiO_2," *Physical Review B*, vol. 61, no. 21, pp. 14414–14419, Jun. 2000, https://doi.org/10.1103/PhysRevB.61.14414.

[30] W. J. Yin, S. Chen, J. H. Yang, X. G. Gong, Y. Yan, and S. H. Wei, "Effective band gap narrowing of anatase TiO2 by strain along a soft crystal direction," *Applied Physics Letters*, vol. 96, no. 22, Jun. 2010, Art. no. 221901, https://doi.org/10.1063/1.3430005.

[31] I. Erdem and H. H. Kart, "Density functional theory study of tin and titanium dioxides: Structural and mechanical properties in the tetragonal rutile phase," *Materials Science in Semiconductor Processing*, vol. 28, pp. 59–65, Dec. 2014, https://doi.org/10.1016/j.mssp.2014.05.037.

[32] D. O. Scanlon *et al.*, "Band alignment of rutile and anatase TiO2," *Nature Materials*, vol. 12, no. 9, pp. 798–801, Sep. 2013, https://doi.org/10.1038/nmat3697.

[33] A. Jain *et al.*, "A high-throughput infrastructure for density functional theory calculations," *Computational Materials Science*, vol. 50, no. 8, pp. 2295–2310, Jun. 2011, https://doi.org/10.1016/j.commatsci.2011.02.023.

[34] A. Jain *et al.*, "Formation enthalpies by mixing GGA and GGA +U calculations," *Physical Review B*, vol. 84, no. 4, Jul. 2011, Art. no. 045115, https://doi.org/10.1103/PhysRevB.84.045115.

[35] P. Borlido, J. Schmidt, A. W. Huran, F. Tran, M. A. L. Marques, and S. Botti, "Exchange-correlation functionals for band gaps of solids: benchmark, reparametrization and machine learning," *npj Computational Materials*, vol. 6, no. 1, Jul. 2020, Art. no. 96, https://doi.org/10.1038/s41524-020-00360-0.

[36] V. P. Zhukov and E. V. Chulkov, "Ab initio approach to the excited electron dynamics in rutile and anatase TiO_2," *Journal of Physics: Condensed Matter*, vol. 22, no. 43, Jul. 2010, Art. no. 435802, https://doi.org/10.1088/0953-8984/22/43/435802.

[37] S. D. Mo and W. Y. Ching, "Electronic and optical properties of three phases of titanium dioxide: Rutile, anatase, and brookite," *Physical Review B*, vol. 51, no. 19, pp. 13023–13032, May 1995, https://doi.org/10.1103/PhysRevB.51.13023.